PHYSICAL REVIEW E **91**, 060101(R) (2015)

Weightless experiments to probe universality of fluid critical behavior

C. Lecoutre,[1,2,*] R. Guillaument,[1,2] S. Marre,[1,2] Y. Garrabos,[1,2] D. Beysens,[3,4] and I. Hahn[5]

[1]*CNRS, ICMCB, ESEME, UPR 9048, F-33600 Pessac, France*

[2]*Université Bordeaux, ICMCB, UPR 9048, F-33600 Pessac, France*

[3]*Physique et Mécanique des Milieux Hétérogènes, UMR 7636 CNRS - ESPCI - Université Pierre et Marie Curie - Université Paris Diderot, 10 rue Vauquelin, 75005 Paris, France*

[4]*Service des Basses Températures, CEA-Grenoble & Université Joseph Fourier, F-38000 Grenoble, France*

[5]*Jet Propulsion Laboratory, California Institute of Technology, California 91109, USA*

(Received 30 March 2015; published 8 June 2015)

Near the critical point of fluids, critical opalescence results in light attenuation, or turbidity increase, that can be used to probe the universality of critical behavior. Turbidity measurements in SF_6 under weightlessness conditions on board the International Space Station are performed to appraise such behavior in terms of both temperature and density distances from the critical point. Data are obtained in a temperature range, far (1 K) from and extremely close (a few μK) to the phase transition, unattainable from previous experiments on Earth. Data are analyzed with renormalization-group matching classical-to-critical crossover models of the universal equation of state. It results that the data in the unexplored region, which is a minute deviant from the critical density value, still show adverse effects for testing the true asymptotic nature of the critical point phenomena.

DOI: 10.1103/PhysRevE.91.060101 PACS number(s): 64.60.fd, 05.70.Jk, 78.35.+c, 81.70.Ha

Thermodynamic and transport properties show singularities asymptotically close to the critical points of many different systems. The current theoretical paradigm on critical phenomena using the renormalization-group (RG) approach [1] has ordered these systems in well-defined universality classes [2] and has characterized the asymptotic singularities in terms of power laws of only two relevant scaling fields [3]. The modern theory of critical phenomena has been reasonably well validated in earlier experimental studies, in particular along the so-called critical paths where one expects that only a single field variable determines the distance to the critical point [see, for example, the studies of the specific heat singular behaviors in Refs. [4,5] for the $O(1)$ and $O(2)$ universality classes [6], respectively]. Simultaneously, the quest for such a *true asymptotic* behavior has been a conundrum to the experimentalists performing experiments closer and closer to the critical point, especially for the case of the gas-liquid critical point of simple fluid systems. For example, gravity effects on Earth bound experiment and long density equilibration times are some of the encountered experimental difficulties in studying the fluid's asymptotic critical behavior [7], which belongs to the universality class of the $(N = 1)$-vector model of three-dimensional (3D) Ising-like systems and the $O(1)$ symmetric $(\Phi^2)^2$ field theory [2,6,8]. In fact, Earth-based experiments are typically restricted to a temperature range $\Delta\tau^* = \frac{T}{T_c} - 1 \geqslant 10^{-4}$, with (T_c) T being the (critical) temperature. In this situation, the analytical backgrounds and the classical-to-critical crossover behavior due to the mean-field-like critical point further hindered the test of the asymptotic Ising-like fluid behavior. Such difficulties are intrinsically unavoidable, even along the true critical paths where the crossover contribution due to one additional irrelevant field [9] can be accounted for correctly in the field theory framework [10,11]. This intrinsic difficulty associated with the above limited finite-temperature range has been shown in the recent reanalysis of critical xenon data [12] from the Earth's experiment performed by Güttinger and Cannell [13].

Practically, the experiments performed even in microgravity environments to avoid gravity effects are never exactly on these critical paths. Even though the temperature can be made much closer to T_c, the mean density of the fluid cell is never at its exact critical density value. The error bar related to this latter critical parameter was never contributing to the discussion of the results in terms of true experimental distance to the critical point. As a result, the experimental control of the exact value of the second relevant field was never carefully accounted for in the expected asymptotic Ising-like behavior of the fluid in the close vicinity of its gas-liquid critical point. For instance, in our previous light transmission and turbidity (τ) measurements [14] performed in near-critical SF_6 under microgravity environments, it was noted that the finite small value ($\sim$0.8%) of the off-density criticality could be one of the explanations of the increasing small differences between the experimental data and the theoretical estimates, referred to as the Ornstein-Zernike (OZ) theory [15] along the critical isochoric path.

Here we probe critical point universality along a noncritical path by using over 300 data points obtained in 12 runs of near-critical SF_6 turbidity measurements in weightless condition. More precisely, the 327 new turbidity data were obtained from March 2011 to February 2014 using the SF_6 sample at constant ($\sim$1%) off-critical, liquidlike density (see below) of the ALI insert in the CNES NASA DECLIC facility onboard the International Space Station (ISS). This cell was purposefully filled at a slightly liquidlike density to study boiling phenomena in the two-phase range (see [16] for details), using thus the benefit of the liquid wettability on the cell walls and sapphire windows. Nonetheless, the light transmission and τ measurements on the one-phase domain have provided

*Corresponding author: carole.lecoutre@icmcb.cnrs.fr

a unique set of data valuable to check our approach of the theoretical estimates referring to the fluid singular behavior along a noncritical path. The DECLIC instrument [17] is an advanced optical, thermal, and mechanical facility that uses different inserts dedicated to the studies, without the gravity effects, of the critical point phenomena and the boiling, the solvation-precipitation, and the solidification mechanisms in transparent media.

The ALI DECLIC turbidity measurements were performed very close to the critical point, nearly three orders of magnitude in temperature distance beyond what has been achieved previously on Earth, by taking advantages of the high-level performances of the facility. These turbidity measurements along a noncritical path, comparable to the ones reported in Ref. [14], can now be analyzed with a much improved theoretical understanding over earlier OZ framework studies. The two data sets are in fact different and independently essential in testing our crossover models of the equation-of-state [12] based on the RG approaches of the critical phenomena universality. Indeed, the crossover parametric model (CPM) [18] of the equation of state, although phenomenological, presents the main advantage in calculating the singular thermodynamic properties in any point of the density-temperature phase surface in the close vicinity of the gas-liquid critical point. Despite small numerical differences between universal quantities, the massive renormalization crossover functions and CPM both showed similar Ising-like critical behaviors, only characterized by three fluid-dependent parameters (*de facto* Ising-like in nature). Moreover, it was also shown in the critical xenon case [12] that the CPM can be modified into the crossover master model (CMM) with no adjustable Ising-like critical parameter since the phenomenological master forms of the crossover functions and the CMM only involve the known critical point coordinates [11]. The CMM can then also be used to predict the asymptotic singular behaviors in the near-critical phase region surrounding a well-localized gas-liquid critical point of any one-component fluid.

Turbidity measurements. We briefly recall that the ALI DECLIC turbidity experiments used the attenuation of the intensity of the DECLIC laser light (wavelength $\lambda_0 = 632.8$ nm, focal beam size 0.3 mm, and maximum attenuation of 1-mW power), crossing the central axis of the direct observation cell (DOC) of the ALI insert. Therefore, $\tau_{\text{expt}} = -\frac{\ln(R_I)}{e} + B_\tau$ expresses the light intensity attenuation per unit length through the measurements of the intensity ratio $R_I = I_2/I_1$, where I_1 is the incident laser light intensity from the entrance optics, I_2 is the related transmitted one through the fluid layer, e is the fluid layer thickness, and B_τ is an adjustable constant that accounts for components in the optical path ($B_\tau \simeq 100 \pm 0.5$ m^{-1} for the DECLIC optical design). The DOC (ten years old at near-critical density filling) was described in [16]. Three main DOC characteristics are of present interest. (i) The DOC has a fixed cylindrical-like fluid volume of $D = 10.6$ mm in diameter and $e = 4.115$ mm in thickness. (ii) The fluid under study was SF_6 of electronic quality, corresponding to a 99.98% purity (from Alpha Gaz, Air Liquide). (ii) The DOC was initially filled at a mean liquidlike density $\langle\rho\rangle$, i.e., $\langle\rho\rangle > \rho_c$, with well-controlled relative off-critical density $\langle\delta\tilde{\rho}\rangle = \frac{\langle\rho\rangle}{\rho_c} - 1 = (1 \pm 0.2)\%$ from Earth-based filling and checking processes. This last point will be detailed in a separate analysis including recent postflight data.

The laser light transmission measurements were also used to determine the relative coexistence temperature $T_{\text{coex}} < T_c$. The temperature difference $T_c - T_{\text{coex}} \simeq 55$ μK was estimated using the power law $\Delta\tilde{\rho}_{LV} = B(\Delta\tau^*)^\beta$ describing the symmetrized top of the coexistence curve, with $\Delta\tilde{\rho}_{LV} = \langle\delta\tilde{\rho}\rangle$ and $\Delta\tilde{\rho}_{LV} = \frac{\rho_L - \rho_V}{2\rho_c}$, $B = 1.596$, $\beta = 0.325\,75$, and $T_c(SF_6) = 318\,733.000$ mK [14]. Here ρ_L and ρ_V are the coexisting liquid and vapor densities, respectively. Note that the absolute calibration of the temperature sensors of the thermostat was not required to determine $T_{\text{coex}}(SF_6)_{\text{ALI}}$, which can then be used as a relative reference for the temperature scale associated with the ALI DECLIC setup. In this case, the thermal monitoring by the DECLIC facility gives a relative temperature uncertainty of the order of 15 μK, with a temperature resolution of 1 μK over the complete duration of the experimental run. Therefore, our turbidity data were obtained from a few μK to 1 K above T_{coex} (i.e., $10^{-7} \leqslant \Delta\tau^*_{\text{coex}} = \frac{T}{T_{\text{coex}}} - 1 \leqslant 3.1 \times 10^{-3}$). Note that the methodology for performing these ALI DECLIC turbidity experiments remains similar to the one for ALICE2 experiments in the MIR station (see Ref. [14]). The major improvement results from the use of an upgraded temperature timeline in DECLIC, which has greatly benefited from the CADMOS and NASA teleoperational managing of this facility. That was especially noticeable over the (at least) 2-d duration of the final part of the timeline where the last decade $T - T_{\text{coex}} \leqslant 1.2$ mK was covered by performing a series of -100-μK temperature depth quenches, of at least 4-h relaxation period each. Therefore, by combining the μK resolution with the 15-μK uncertainty, a typical error bar of 30 μK can be attributed to the data point in the closest temperature range. A detailed description of this preparation of a homogeneous thermodynamic state of a near-critical fluid sample in weightlessness conditions at the closest temperature above the two phase domain (i.e., a few μK to $\sim$50 μK above T_{coex}, typically) is beyond the scope of the present paper.

Our 327 τ_{expt} data are reported as functions of $T - T_{\text{coex}}$ in Fig. 1, noting that 85 data are in the range $T - T_{\text{coex}} \leqslant 1$ mK and that the temperature range not affected by gravity in a similar Earth experiment is restricted to $T - T_{\text{coex}} \geqslant 38$ mK [19]. The symbols defined in the legend of Fig. 1 correspond to the 12 series of ALI DECLIC turbidity data. Each series corresponds to a typical, about 5-d-duration, temperature timeline, performed during the different sequences, which covers the temperature range $T_{\text{coex}} + 1$ K $\rightarrow T_{\text{coex}}$. In Fig. 1 we have also added our previous turbidity data (in the form of red closed circles) obtained from the ALICE2 turbidity experiments [14], using a cell with off-critical density $\langle\delta\tilde{\rho}\rangle_{\text{ALICE2}} = (0.8 \pm 0.1)\%$.

Turbidity functional forms for a near-critical fluid. Turbidity of a fluid close to its gas-liquid critical point is most essentially due to Rayleigh light scattering by density fluctuations. Measurements of τ as a function of the distance from the critical point allow Ising-like asymptotic formulations for the static isothermal compressibility (κ_T, governed by the critical exponent γ along the critical isochore) and the correlation length (ξ, governed by the critical exponent ν along the critical isochore) to be checked. Indeed, from the detailed

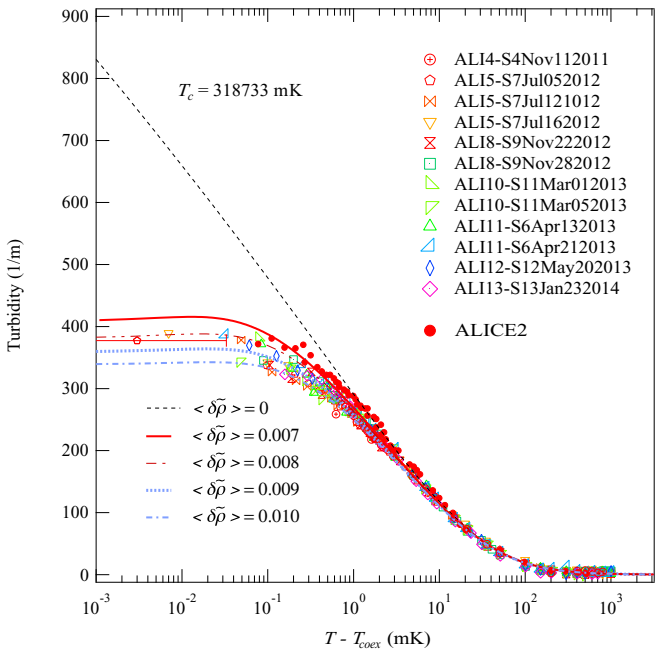

FIG. 1. (Color online) A lin-log plot of turbidity τ (expressed in m^{-1}) as a function of $T - T_{coex}$ (expressed in mK) obtained from the present ALI DECLIC and previous ALICE2 light transmission measurements in SF_6 (symbols are defined in the legend) and compared to the predicted turbidity from Eq. (2), using the CMM equation-of-state model with calculated parameters from column 3 of Table I. The black dashed curve represents Eq. (2) for $\langle\delta\tilde{\rho}\rangle = 0$ (exact critical isochore). The additional four (red solid, red double-dot–dashed, blue dotted, blue dot-dashed) curves represent Eq. (2) for $\langle\delta\tilde{\rho}\rangle$ covering the 0.7%–1.0% range, by using 0.1% steps, respectively. The typical 30-μK temperature error bar is only indicated by a horizontal red bar for the closest data point ($T - T_{coex} \sim 3\ \mu$K).

analysis given in [12], τ can be written in the scaling form

$$\tau = \frac{\pi A_0 k_B T \kappa_T}{y^2} H(\eta, y), \tag{1}$$

where $A_0 = \frac{\pi^2}{\lambda_0^4}[\frac{(n^2-1)(n^2+2)}{3}]^2$, n is the fluid refractive index, k_B is the Boltzmann constant, $y = k_0\xi$ is universal (independent of the normalization), $k_0 = \frac{2\pi n}{\lambda_0}$ is the amplitude of the incident light wave vector ($\sim 10^{-7}$ m^{-1} for $\lambda_0 \sim 632.8$ nm), and $H(\eta, y)$ is the turbidity scaling function, which is universal as y is, the critical exponent η satisfying thus the hyperscaling law $\gamma = 2\nu - \eta\nu$. As shown in [12], when $T \to T_c$, i.e. $y \gg 1$ or $x \to \infty$, only the asymptotic critical behavior of $H(\eta, y)$ must be explicitly a function of the critical exponent η. In terms of the usual Ising-like power law along the critical isochore, i.e., for $y \gg 1$ and $\Delta\tau^* \to 0$, $H(\eta, y) \propto F \times (\Delta\tau^*)^{-\eta\nu}$, where F is a universal quantity. Thus F is related to the saturated finite turbidity at the exact critical point, such as $\tau \sim \frac{cte}{\eta}$, as shown by the asymptotic analysis of Ferrell [20]. However, Ferrell's asymptotic analysis, as well as its confirmation by the Monte Carlo simulation of a simple cubic Ising lattice by Martin-Mayor *et al.* [21], leads to Ising-like limiting forms of the turbidity expected to be valid only for $\Delta\tau^* < 10^{-5}$, i.e., very close to the critical temperature. At large distance from T_c, when $x \leqslant 1$, the turbidity reduces to Puglielli and Ford's [19] estimation from the OZ theory. In such a second limiting case, Eq. (1) takes the practical functional form $\tau_{PF} = \frac{\pi A_0 k_B T \kappa_T}{y^2} H_{PF}(y)$, with $H_{PF}(y) = \frac{1}{8y^4}[(8y^4 + 4y^2 + 1)\ln(1 + 4y^2) - 4y^2(1 + 2y^2)]$. The ratio $\frac{H_{PF}(y)}{y^2}$ reaches the constant value $\frac{8}{3}$ for $y \ll 1$, leading to $\tau_{PF} = \tau_0(1 + \Delta\tau^*)(\Delta\tau^*)^{-\gamma} \propto T\kappa_T$ far away from T_c. Here $\tau_0 = \pi A_0 k_B T_c \Gamma_0^+$ is a temperature-independent quantity, only proportional to the leading amplitude Γ_0^+ of the singular behavior of $\chi_T^* = \kappa_T p_c$, where p_c is the critical pressure. Unfortunately, for a 3D Ising system, $H(\eta, y)$ always remains unknown between the above two limiting behaviors. Therefore, in our modeling we consider the phenomenological fitting formulation proposed by Martin-Mayor *et al.* [21] to reproduce the crossover between the turbidity results of the Monte Carlo simulation (close to T_c) and the ones of the PF approximation (far from T_c), such as

$$\tau_{MM,fit} = \tau_{PF}[0.666\,421 + 0.242\,339(1 + 0.008\,793\,6y^2)^{\eta/2} + 0.091\,180\,1(1 + 0.09y^4)^{\eta/4}]. \tag{2}$$

This fitting form recovers the condition $\tau_{MM,fit} \sim \tau_{PF}$ far from the critical temperature ($y \leqslant 1$ or $\Delta\tau^* \geqslant 10^{-5}$).

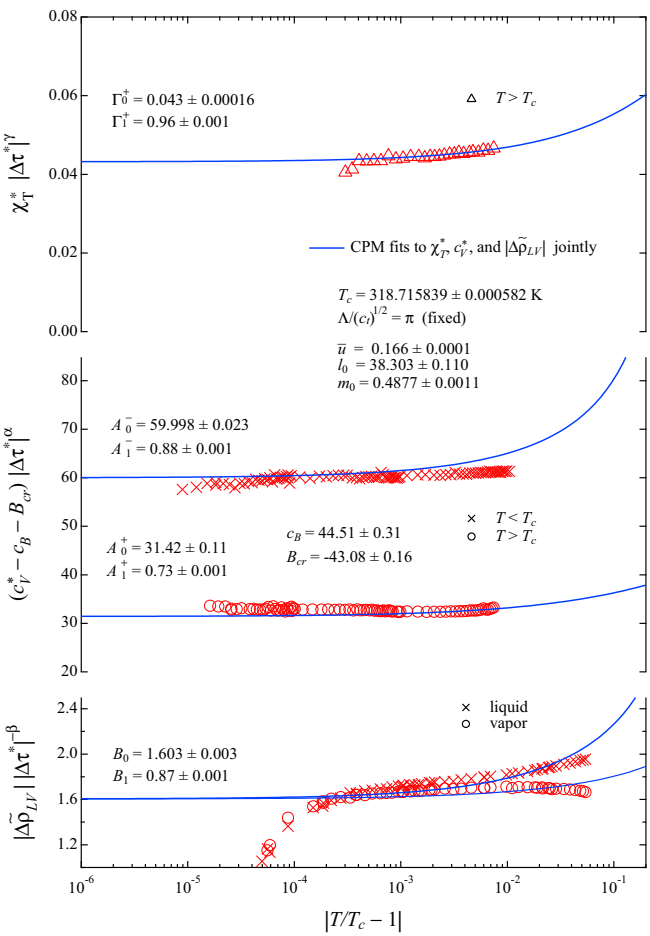

FIG. 2. (Color online) Joint fit result for the free parameters l_0, m_0, and $\bar{u}$ of the CPM fitting the SF_6 $\chi_T^* = \kappa_T p_c$, c_V^*, and $\Delta\tilde{\rho}_{LV}$ measurements of Refs. [22], [4], and [23], respectively, as functions of $|\Delta\tau^*|$ along the critical isochore (see Ref. [18] for the amplitude notation and inserted labels for the curves and the symbols).

TABLE I. Sulfurhexafluoride values of the Ising-like parameters l_0, m_0, and $\bar{u}$ for the CPM joint fit (see Fig. 2), the CMM [see Eq. (3) and the text], and fitting the turbidity data with $\bar{u} = 0.166$, $\Lambda/(c_t)^{1/2} = \pi$ (fixed), and l_0, m_0, and $\langle\delta\tilde{\rho}\rangle$ as free parameters (see the text).

SF_6	CPM joint fit	CMM	Turbidity fit (this work)
l_0	38.303 ± 0.110	36.1923	36.472±0.694
m_0	0.4877 ± 0.001	0.48568	0.4915±0.001
$\bar{u}$	0.166 ± 0.0001	0.124284	0.166 (fixed)
$\Lambda/(c_t)^{1/2}$	π (fixed)	π (fixed)	$\langle\delta\tilde{\rho}\rangle_{\rm ALI} = (0.95 \pm 0.05)\%$
$g^{1/2}$	0.5215 ± 0.0001	0.39045	$\langle\delta\tilde{\rho}\rangle_{\rm ALICE2} = (0.75 \pm 0.17)\%$

Estimations of ξ, κ_T, and τ for near-critical SF_6. Our calculations of $\kappa_T(\Delta\tau^*, \langle\delta\tilde{\rho}\rangle)$, $\xi(\Delta\tau^*, \langle\delta\tilde{\rho}\rangle)$, and $\tau(\Delta\tau^*, \langle\delta\tilde{\rho}\rangle)$ for the near-critical ($\langle\delta\tilde{\rho}\rangle \neq 0$) SF_6 case are similar to the critical ($\langle\delta\tilde{\rho}\rangle = 0$) Xe case reported in [12]. First, the CPM free adjustable parameters (l_0, m_0, and $\bar{u}$) for SF_6 are obtained from a joint fitting of isothermal compressibility [22], heat capacity at constant volume [4], and coexisting density curve [23]. The results are shown in Fig. 2, where only the reduced temperature range of the c_V data obtained in microgravity reaches the 10^{-5}–10^{-4} decade. Second, the corresponding CMM fixed parameters are obtained from the relations [12]

$$l_0 = \frac{3.383\,17}{\mathcal{Z}_\chi^+}\frac{\mathcal{Z}_M}{3.286\,13}(Z_c)^{1/2}(Y_c)^{\beta+\gamma},$$
$$m_0 = \frac{\mathcal{Z}_M}{3.286\,13}(Z_c)^{-1/2}(Y_c)^{\beta}, \quad (3)$$
$$[\bar{u}\pi]^{-2\Delta_s}(1-\bar{u}) = \frac{\mathcal{Z}_\varkappa^{1+}}{0.590}(Y_c)^{\Delta}$$

neglecting quantum effects for the SF_6 case and using the arbitrary relation $\frac{\Lambda}{(c_t)^{1/2}} = \pi$ initially adopted by the authors in Ref. [18]. Here $\mathcal{Z}_\chi^+ = 0.11975$, $\mathcal{Z}_M = 0.4665$, and $\mathcal{Z}_\varkappa^{1+} = 0.555$ [11], while $Z_c = p_c m/(k_B \rho_c T_c) = 0.2795$ and $Y_c = (T_c/p_c)\gamma_c' - 1 = 6.0896$ [14] are the two scale-factors estimated from the generalized critical coordinates of SF_6 (m is the molecular mass and γ_c' is the common critical slope, in the p,T diagram, of the critical isochore and the saturation pressure curve at the critical point). Table I shows that the free (column 2) and fixed (column 3) values are in close agreement.

Our theoretical estimation of τ using Eq. (2) with CMM parameters (column 3, Table I) to calculate ξ and κ_T for $\langle\delta\tilde{\rho}\rangle = 0$ corresponds to the black dashed curve on a log-lin scale in Fig. 1. The additional four curves correspond to the similar predictive modeling for four near-critical isochores covering the $\langle\delta\tilde{\rho}\rangle = 0.7\%$–$1.0\%$ range, using four 0.1% steps (see the legend in Fig. 1). This $\langle\delta\tilde{\rho}\rangle$ range includes the experimental central values $\langle\delta\tilde{\rho}\rangle_{\rm ALI} = 1\%$ and $\langle\delta\tilde{\rho}\rangle_{\rm ALICE2} = 0.8\%$.

Discussion. Figure 1 indicates that the τ calculations from Eq. (2), without adjustable parameters, are in agreement with our experimental data using $\langle\delta\tilde{\rho}\rangle \approx 0.9\%$ (blue dotted curve) for the present ALI DECLIC case and $\langle\delta\tilde{\rho}\rangle \approx 0.7\%$ (red solid curve) for the previous ALICE2 case. This good agreement is noticeable in the temperature range $T - T_{\rm coex} \lesssim 25$ mK, investigated experimentally now as a function of $\langle\delta\tilde{\rho}\rangle$, whereas the estimated small differences (∼0.1%) from the above central values are of the same order of magnitude as the experimental error bar. In addition, complementary fits of the τ data (ALI DECLIC plus ALICE2), fixing $\bar{u} = 0.166$ (joint fit value) with l_0, m_0, and $\langle\delta\tilde{\rho}\rangle$ as the free parameters, lead to the results reported in column 4 of Table I. The l_0 and m_0 differences from column 2 could be easily understood by considering the limited available data range of the joint fit compared to the one of the turbidity data. Similarly, the $\langle\delta\tilde{\rho}\rangle$ values agree with an uncertainty of ∼0.1%.

The current analysis shows that the off-critical density of the cell is the dominant effect that explains the observed increasing deviation from the critical singular behavior of the turbidity approaching T_c. This conclusion benefits from the microgravity environment and the high-level capabilities of ALI DECLIC for experimenting accurately at temperature distances closer than 1 mK from $T_{\rm coex}$. The multiple-scattering effect is considered to be a negligible factor (<10%) in our forward-scattering case ($\theta < 2.7^\circ$) [24]. The intrinsic gravitational effects in the sample fluid at the size of the laser beam, which could limit the growth of the correlation length on Earth, are also insignificant in microgravity conditions even at the reduced temperature of 10^{-7} [7].

The modeling of τ is comparable (in amplitude and uncertainty) to the three sets of Ising-like parameters given in Table I. In addition, the estimated values of the cell densities are in agreement with Earth-based experimental determinations. Finally, in a temperature-density range very close to ρ_c and T_c, the turbidity behavior is reasonably well understood from the use of the parametric form of the equation of state without any adjustable parameter. This modeling approach is made in conformity with the Ising-like universality features of the massive renormalization scheme, only knowing the SF_6 generalized critical coordinates.

We thank the DECLIC CNES-NASA teams, and associated industrial teams, involved in the ALI-DECLIC project development and achievement and in particular the NASA and CADMOS teams for operational managing and control of the facility onboard the ISS. C.L., R.G., S.M., Y.G., and D.B. are grateful to CNES for financial support. The research of I.H. was carried out at Jet Propulsion Laboratory, California Institute of Technology, under a contract with NASA.

[1] K. G. Wilson, Rev. Mod. Phys. **47**, 773 (1975).
[2] J. Zinn-Justin, *Quantum Field Theory and Critical Phenomena*, 4th ed. (Clarendon, Oxford, 2002).
[3] M. E. Fisher, J. Math. Phys. **5**, 944 (1964).
[4] A. Haupt and J. Straub, Phys. Rev. E **59**, 1795 (1999).
[5] J. A. Lipa, D. R. Swanson, J. A. Nissen, Z. K. Geng, P. R. Williamson, D. A. Stricker, T. C. P. Chui, U. E. Israelsson, and M. Larson, Phys. Rev. Lett. **84**, 4894 (2000).
[6] M. Barmatz, I. Hahn, J. A. Lipa, and R. V. Duncan, Rev. Mod. Phys. **79**, 1 (2007).

[7] M. R. Moldover, J. V. Sengers, R. W. Gammon, and R. J. Hocken, Rev. Mod. Phys. **51**, 79 (1979).
[8] M. A. Anisimov and J. V. Sengers, in *Equations of State for Fluids and Fluid Mixtures*, edited by J. V. Sengers, R. F. Kayser, C. J. Peters, and H. J. White, Jr. (Elsevier, Amsterdam, UK, 2000), pp. 381–434, and references therein.
[9] F. J. Wegner, Phys. Rev. B **5**, 4529 (1972).
[10] C. Bagnuls and C. Bervillier, Phys. Rev. E **65**, 066132 (2002).
[11] Y. Garrabos, C. Lecoutre, F. Palencia, B. Le Neindre, and C. Erkey, Phys. Rev. E **77**, 021116 (2008).
[12] Y. Garrabos, C. Lecoutre, S. Marre, D. Beysens, and I. Hahn, J. Stat. Phys. **158**, 1379 (2015).
[13] H. Güttinger and D. S. Cannell, Phys. Rev. A **24**, 3188 (1981).
[14] C. Lecoutre, Y. Garrabos, E. Georgin, F. Palencia, and D. Beysens, Int. J. Thermophys. **30**, 810 (2009).
[15] L. S. Ornstein and F. Zernike, Proc. Acad. Sci. Amsterdam **17**, 793 (1914); Phys. Z. **19**, 134 (1918).
[16] Y. Garrabos, C. Lecoutre, D. Beysens, V. Nikolayev, S. Barde, G. Pont, and B. Zappoli, Acta Astronaut. **66**, 760 (2010).
[17] See http://smsc.cnes.fr/DECLIC/index.htm.
[18] V. A. Agayan, M. A. Anisimov, and J. V. Sengers, Phys. Rev. E **64**, 026125 (2001).
[19] V. G. Puglielli and N. C. Ford, Phys. Rev. Lett. **25**, 143 (1970).
[20] R. A. Ferrell, Phys. A **177**, 201 (1991).
[21] V. Martin-Mayor, A. Pelissetto, and E. Vicari, Phys. Rev. E **66**, 026112 (2002).
[22] G. T. Feke, G. A. Hawkins, J. B. Lastovka, and G. B. Benedek, Phys. Rev. Lett. **27**, 1780 (1971).
[23] J. Weiner, Ph.D. thesis, University of Massachusetts, Amherst, 1974.
[24] A. E. Bailey and D. S. Cannell, Phys. Rev. E **50**, 4853 (1994).